

Exploring Explicit Domain Supervision for Latent Space Disentanglement in Unpaired Image-to-Image Translation

Jianxin Lin, Zhibo Chen, *Senior Member, IEEE*, Yingce Xia, Sen Liu,
Tao Qin, and Jiebo Luo, *Fellow, IEEE*

Abstract—Image-to-image translation tasks have been widely investigated with Generative Adversarial Networks (GANs). However, existing approaches are mostly designed in an unsupervised manner while little attention has been paid to domain information within unpaired data. In this paper, we treat domain information as explicit supervision and design an unpaired image-to-image translation framework, **Domain-supervised GAN (DosGAN)**, which takes the first step towards the exploration of explicit domain supervision. In contrast to representing domain characteristics using different generators or domain codes, we pre-train a classification network to explicitly classify the domain of an image. After pre-training, this network is used to extract the domain-specific features of each image. Such features, together with the domain-independent features extracted by another encoder (shared across different domains), are used to generate image in target domain. Extensive experiments on multiple facial attribute translation, multiple identity translation, multiple season translation and conditional edges-to-shoes/handbags demonstrate the effectiveness of our method. In addition, we can transfer the domain-specific feature extractor obtained on the Facescrub dataset with domain supervision information to unseen domains, such as faces in the CelebA dataset. We also succeed in achieving conditional translation with any two images in CelebA, while previous models like StarGAN cannot handle this task.

Index Terms—Image-to-image translation, explicit domain supervision, generative adversarial networks.

1 INTRODUCTION

Image-to-image translation covers a wide variety of computer vision problems, including image stylization [1], segmentation [2] and image super-resolution [3]. It aims at learning a mapping that can convert an image from a source domain to a target domain, while preserving the main presentations of the input images. For example, in the aforementioned three tasks, an input image might be converted to a portrait similar to Van Gogh's styles, a segmentation map splitted into different regions, or a high-resolution image, while the content remains unchanged. Since it is usually challenging to collect a large amount of paired data for such tasks, unsupervised learning algorithms have been widely adopted in image-to-image translation models. Particularly, the generative adversarial networks (GAN) [4] and dual learning [5] are studied. One of the most popular model, **CycleGAN** [6], tackles cross-domain unpaired image-to-image translation by the aforementioned two techniques, where the GANs are used to ensure the generated images belonging to the target domain, and dual learning can help improve image qualities by minimizing reconstruction loss.

- Zhibo Chen (*Corresponding Author*), Jianxin Lin and Sen Liu are with University of Science and Technology of China, Hefei, Anhui, 230026, China, (e-mail: chenzhibo@ustc.edu.cn).
- Yingce Xia and Tao Qin are with Microsoft Research Asia, Beijing, 100080, China, (e-mail: Yingce.Xia@microsoft.com and taoqin@microsoft.com).
- Jiebo Luo is with the Department of Computer Science, University of Rochester, Rochester, NY 14627 USA, (e-mail: jiebo.luo@gmail.com).

This work was supported in part by NSFC under Grant 61571413, 61632001.

An implicit assumption of image-to-image translation is that an image contains two kinds of features¹ [7], [8], [9]: domain-independent features, which are preserved during the translation (i.e., the content when translating a natural image to Van Gogh' styles), and domain-specific features, which are changed during the translation (i.e., the styles when translating the image to Van Gogh' styles). **Image-to-image translation** aims at transferring images from the source domain to the target domain by preserving domain-independent features while replacing domain-specific features. Therefore, the extraction of domain-specific features plays an important role for image-to-image translation. There are three main challenges in solving the image-to-image translation problem. The first one is how to extract the domain-independent and domain-specific features for a given image. The second is how to merge the features from two different domains into a natural image in the target domain. The third one is that there is no paired data for us to learn such the mappings. In this paper, we focus on solving image-to-image translation problems with latent space disentanglement.

Although it is difficult to obtain the paired data across different image domains, we observe that in many cases, we are aware which domain an image comes from [10], [11]. Motivated by this observation, we propose to use this domain-level signal as explicit supervision and pre-train a deep convolutional neural network (CNN) to predict

¹ Note that the two kinds of features are relative concepts, and domain-specific features in one task might be domain-independent features in another task, depending on what domains one focuses on in the task.

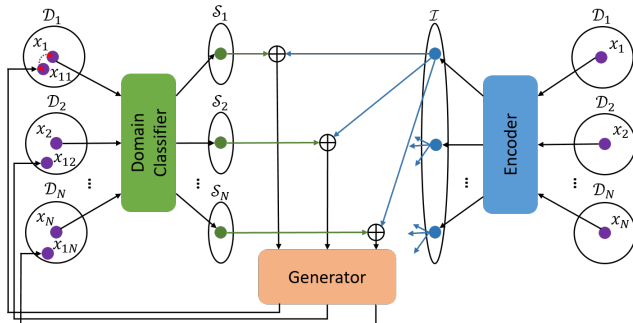


Fig. 1. The basic idea of our DosGAN-c on conditional image-to-image translation. $\mathcal{D}_k \forall k \in [N]$ are N domains of interests. Our model disentangles N domain-specific feature latent space S_k through a classifier. Encoder in DosGAN-c learns to project images from N domains to a domain-independent latent space I shared by all domains. Given $x_1 \in \mathcal{D}_1$ for example, various translation image x_{1k} can be obtained by varying domain-specific features in S_k . Specially, x_{11} should be consistent with x_1 .

which domain an image is from. If such a network can well differentiate images from different domains, the output of the second-to-last layer of the network should carry rich domain information which captures each domain's specific characteristic. Therefore, we can leverage such a pre-trained CNN to extract the domain-specific features of an image. Compared with works [7], [8], [9] that use two separated domain-specific feature extractors for two domain translation, we utilize the domain classifier as a general domain-specific feature extractor which can be easily generalized to multi-domain translation. With the well-defined domain-specific features, the domain-independent features can be easily obtained by feature disentanglement.

Generally, in this work, we first propose a new framework for common image-to-image translation, which is composed by a domain-specific feature extractor, a domain-independent feature extractor, and an image generator. The domain-specific feature extractor is pre-trained based on domain supervision, and then the domain-independent feature extractor and the generator are trained based on Generative Adversarial Networks (GANs) and dual learning [5]. We choose GAN and dual learning due to the following considerations: (1) The dual learning framework can help learn to extract and merge the domain-specific and domain-independent features by minimizing carefully designed reconstruction errors, including self-reconstruction errors and cross-domain reconstruction errors. (2) GAN can ensure that the generated images well mimic the natural images in the target domain. (3) Both dual learning [5], [6], [12] and GAN [4], [13], [14] work well under unsupervised settings. Therefore, we name this framework as Domain-supervised GAN (briefly, DosGAN).

Existing multi-domain translation models, such as StarGAN, also lack the ability to control the translated results in the target domain and their results usually lack of diversity in the sense that a fixed image usually leads to (almost) deterministic translation result. With two kinds of latent feature (i.e., domain-specific and domain-independent features) disentangled, we can devise a conditional DosGAN (briefly, DosGAN-c) for conditional image-to-image translation [7], which is to translate an image from the source

domain to the target domain conditioned on a given image in the target domain and requires that the generated image should inherit some domain-specific features of the conditional image from the target domain. The DosGAN-c shares the same network architecture with DosGAN, and the difference between two frameworks only lies in the inputs and losses.

Compared with the previous work cd-GAN [7], there are three main differences: (1) Unlike cd-GAN or CycleGAN that simply treats multiple domains as different sources of images, in this work, we regard domain information as explicit supervision, where we train a classifier to classify the domain of the input image, and convert it to a domain-specific feature extractor. (2) The domain-specific features in our model are explicitly modeled, which are extracted by a well-defined and fixed domain classification network. However, in cd-GAN, no such kind of explicit supervision signal is applied, causing the ambiguity in the extracted feature. (3) In this paper, we generalize the conditional image-to-image translation from two domains (with two models) to multiple domains (≥ 2 domains, with one model only), pushing the frontier of multi-domain conditional image-to-image translation.

We carry out experiments on multiple facial attribute translation, multiple season translation and conditional edges-to-shoes/handbags translation. The results demonstrate that with domain supervision, our approach can better extract domain-specific features and translate images.

Interestingly, we find that the pre-trained domain-specific feature extractor has certain transferability. We transfer the domain-specific feature extractor trained on the Facescrub dataset, where the domain of each image (i.e., the identity of each face image) is known, to the CelebA dataset, where the domain (i.e., identity) of each image is unknown. The two datasets share the same semantic representations (i.e., face images), which provides a viable way to produce the domain-specific features for the faces in the unknown domains. Therefore, we can succeed in achieving conditional translation on CelebA by transferring the pre-trained domain-specific feature extractor, while previous methods cannot.

Our main contributions can be summarized as follows:

- We explicitly exploit domain supervision in unpaired image-to-image translation by extracting well-defined domain-specific features through a simple domain classifier.
- We disentangle two latent features by explicitly utilizing domain supervision and achieve performances better than several strong baseline methods.
- We show that the pre-trained domain-specific feature extractor can be transferred across datasets, which has not been investigated before.

The remaining parts of this paper are organized as follows. We review related work in Section 2 and present our approach in Section 3. The experimental results are reported in Section 4. We conclude our work and discuss several future directions in the last section. Our code is publicly available to the research community at <https://github.com/linjx-ustc1106/DosGAN-PyTorch>.

149

2 RELATED WORKS

Generative modeling. Image generation has been widely explored in recent years, and works have been putting effort on modeling the natural image distribution. This problem was initially solved by Boltzmann machines [15] and autoencoders [16], [17]. Variational autoencoder (VAE) [18] aims to improve the quality and efficiency of image generation by reparametrization of a latent distribution. GAN [4] was firstly proposed to generate images from random variables by a two-player minimax game. Various works have been proposed to exploit the capability of GAN for various image generation tasks. InfoGAN [19] learns to disentangle latent representations by maximizing the mutual information between a small subset of the latent variables and the observation. Radford et al. [13] presented a class of deep convolutional generative networks (DCGANs) for high-quality image generation and unsupervised image classification tasks, which bridges the gap between convolutional neural networks (CNNs) and unsupervised image generation.

Supervised image-to-image translation. The supervised image-to-image translation aims to learn a parametric translation function that transforms an input image in a source domain to an image in a target domain when paired data is available. Many computer vision tasks can be posed as this problem. For example, Long et al. [2] proposed a fully convolutional network (FCN) for image-to-segmentation translation. SRGAN [3] maps low-resolution images to high resolution images. Isola et al. [20] proposed a general conditional GAN (pix2pix) for image-to-image translation tasks, including label-to-street scene and aerial-to-map. In order to overcome the limitation of relatively low resolution in pix2pix and lack of realistic details and texture, Wang et al. [21] proposed a HD version of pix2pix which increases the resolution to 2048*1024. In this work, a coarse-to-fine generator, three multi-scale discriminators, and a feature matching loss are utilized. Like prior research [22] attempted to learn disentangled representations, such as content and style, Zhu et al. [23] proposed a BicycleGAN to learn multimodal image-to-image translation by building bijective consistency between output and latent code.

Unpaired image-to-image translation. Since it is usually expensive to collect a large amount of paired data for supervised image-to-image translation tasks, unpaired learning based algorithms have been widely adopted. Based on adversarial training, Dumoulin et al. [24] and Donahue et al. [25] proposed algorithms to jointly learn mappings between latent space and data bidirectionally. Taigman et al. [26] presented a domain transfer network (DTN) for unpaired cross-domain image generation by assuming constant latent space between two domains, which could generate images of target domain's style and preserve their identity. He et al. [5] proposed a dual learning mechanism that can enable a neural machine translation system to automatically learn from unlabeled data through a dual learning game. Inspired by the idea of dual learning, DualGAN [12], DiscoGAN [27] and CycleGAN [6] were proposed to tackle the unpaired image translation problem by training two cross-domain transfer GANs at the same time. To generate controllable translation result, Lin et al. [7] decompose the image latent

space into domain-independent and domain-specific feature spaces, and raise a new problem named as conditional cross-domain translation which can assign domain-specific feature for generated result by feeding a conditional image in the target domain. Similar to [7], other two works [8], [9] proposed to disentangle latent space and generate diverse translation results. Choi et al. [10] further proposed a StarGAN that can perform image-to-image translations for multiple domains using only a single model. Similarly, Liu et al. [11] proposed a UFDN that learns domain-invariant representation from multiple domains and can perform continuous cross-domain image translation and manipulation. Some other works also utilized attention mechanism for more accurate image-to-image translation. DA-GAN [28] firstly finds the instance-level corresponding of two domains in the latent space by introducing attention mechanism, then generates images from the highly-structured latent space. In [29], GANimation is proposed to generate anatomically-aware facial animation. Attention mechanism is exploited to make the scheme more robust and have the capacity of dealing with images in the wild. Authors in [30], [31] introduced attention map to avoid cycle consistency loss distracted by background factors and achieved better performance than original CycleGAN.

3 FRAMEWORK

In this section, we introduce our proposed framework. We first give a general formulation to image translation and conditional image translation, then describe our network architecture, and finally present the training algorithm and discussion.

3.1 Problem formulation

We work on multiple domain translation with one single model, but to increase readability, we will introduce two domain translation between domain A (denoted as \mathcal{D}_A) and domain B (denoted as \mathcal{D}_B). Suppose we have a domain-specific feature extractor $\alpha(\cdot)$ and a domain-independent feature extractor $\beta(\cdot)$.² Given an image $x \in \mathcal{D}_A$ or $x \in \mathcal{D}_B$, we can get its domain-specific features x^s and domain-independent features x^i by applying the two extractors:

$$x^s = \alpha(x), \quad x^i = \beta(x). \quad (1)$$

In this paper, x without any superscript denotes an image. x with superscripts i and s refer to domain-independent features (e.g., x^i) and domain-specific features (e.g., x^s) respectively. Note that the domain-independent features of an image should be kept and its domain-specific features should be changed while translating it from one domain to other domain.

Then the style S_A of \mathcal{D}_A and the style S_B of \mathcal{D}_B are:

$$S_A = \int_{x \in \mathcal{D}_A} \alpha(x)p_A(x)dx, \quad S_B = \int_{x \in \mathcal{D}_B} \alpha(x)p_B(x)dx, \quad (2)$$

where $p_A(x)$ and $p_B(x)$ denote the probabilities of the image x belonging to \mathcal{D}_A and \mathcal{D}_B . Empirically, given a set

²⁰⁷². We will discuss how to learn the two extractors in the following two subsections.

258 D_A of images in domain A (i.e., $D_A \subset \mathcal{D}_A$) and a set of
 259 $D_B \subset \mathcal{D}_B$, S_A and S_B can be estimated through

$$S_A \approx \frac{1}{|D_A|} \sum_{x_A \in D_A} \alpha(x_A); S_B \approx \frac{1}{|D_B|} \sum_{x_B \in D_B} \alpha(x_B), \quad (3)$$

260 where $|D_A|$ and $|D_B|$ refer to the number of images in
 261 D_A and D_B . Let \oplus denote a generator, which takes a
 262 set of domain-specific features x^s and a set of domain-
 263 independent features x^i as inputs and generates an image in
 264 the corresponding domain: for any $x_A \in \mathcal{D}_A$ and $x_B \in \mathcal{D}_B$,

$$x_A = x_A^i \oplus x_A^s, \quad x_B = x_B^i \oplus x_B^s. \quad (4)$$

265 **Definition 1** With the above notations, the translation from
 266 \mathcal{D}_A to \mathcal{D}_B and the translation from \mathcal{D}_B to \mathcal{D}_A can be written
 267 as follows: for any $x_A \in \mathcal{D}_A$ and $x_B \in \mathcal{D}_B$,

$$x_{AB} = x_A^i \oplus S_B, \quad x_{BA} = x_B^i \oplus S_A, \quad (5)$$

268 where x_{AB} and x_{BA} denote the translation result.

269 **Definition 2** The conditional image-to-image translation of
 270 an image x_A in domain A conditioned on an image x_B in
 271 domain B , i.e., $\mathcal{D}_A \times \mathcal{D}_B \mapsto \mathcal{D}_B$, and the dual translation
 272 $\mathcal{D}_B \times \mathcal{D}_A \mapsto \mathcal{D}_A$, can be written as

$$x_{AB} = x_A^i \oplus x_B^s, \quad x_{BA} = x_B^i \oplus x_A^s. \quad (6)$$

273 Different from existing works [7], [8], [9], in this work, the
 274 domain-specific feature extractor $\alpha(\cdot)$ is pre-trained in a
 275 supervised setting based on domain supervision and will
 276 be kept fixed during the training of the translation system.
 277 In the following subsections, we will first discuss how to
 278 pre-train $\alpha(\cdot)$, and then present how to learn the domain-
 279 independent feature extractor $\beta(\cdot)$ and the generator \oplus
 280 from unpaired images for image-to-image translation and
 281 conditional image-to-image translation.

282 3.2 Pre-training of domain-specific feature extractor

283 Very different from previous works [6], [7], which simply
 284 treat multiple domains as different sources of images, in this
 285 work, we regard them as explicit supervision and use them
 286 in a supervised way to learn the domain-specific feature
 287 extractor $\alpha(\cdot)$.

288 Given images from N domains, we train a CNN network
 289 to correctly classify the domain of an image. After training,
 290 if the classifier network can accurately detect the domain
 291 of an image, then the output of the second-to-last layer of
 292 this classifier should well capture the domain information of
 293 this image. Thus, we denote the input layer to the second-
 294 to-last layer of this classifier network as our domain-specific
 295 feature extractor $\alpha(\cdot)$. With this pre-trained $\alpha(\cdot)$, we will
 296 introduce our system architectures for image translation in
 297 the coming subsections.

298 3.3 Architecture for image-to-image translation

299 The architecture of our proposed system for image-to-image
 300 translation is shown in Figure 2. As can be seen, to translate
 301 an image x_A from domain A to domain B , we first apply the
 302 domain-specific feature extractor $\alpha(\cdot)$ over all the images
 303 in domain B and obtain the style feature S_B according to
 304 Eqn (3). Then we apply the domain-independent feature
 305 extractor $\beta(\cdot)$ to x_A and obtain the domain-independent

306 features x_A^i . After that, the generator \oplus takes x_A^i and S_B
 307 as inputs and generates the translation results x_{AB} , i.e.,
 308 $x_{AB} = x_A^i \oplus S_B$. In practice, the generator is modeled
 309 by a neural network and needs to be learned, thus, to be
 310 differentiated from the oracle generator \oplus , we use g to
 311 denote the generator to be learned.

312 **Adversarial loss** Following the idea of GANs, we introduce
 313 a discriminator d , which takes a (real or fake) image as input
 314 and output a probability indicating how likely the input
 315 belongs to a real image domain. We illustrate the objective
 316 function as below:

$$\ell_{\text{GAN}} = \frac{1}{|D_A|} \sum_{x_A \in D_A} \log(d_{\text{adv}}(x_A)) + \log(1 - d_{\text{adv}}(x_{AB})), \quad (7)$$

317 where x_{AB} is defined in Eqn. (5). The $g \circ \beta$ network tries
 318 to fool the discriminators by minimizing ℓ_{GAN} , while the
 319 discriminator tries to differentiate generated images from
 320 real ones by maximizing ℓ_{GAN} .

321 **Domain-specific reconstruction loss** Different from Star-
 322 GAN [10] that requires discriminator d to serve as a classifier
 323 that distinguishes which domain the input belongs to, we
 324 adapt the discriminator d to maximize the mutual informa-
 325 tion between domain-specific features and generated images
 326 as InfoGAN [19]. In this case, the domain-specific feature
 327 reconstruction cost $\ell_{\alpha,r}$ of real images and fake images $\ell_{\alpha,f}$
 328 can be formulated as follows:

$$\begin{aligned} \ell_{\alpha,r} &= \frac{1}{|D_A|} \sum_{x_A \in D_A} [\|d_{\text{feat}}(x_A) - x_A^s\|_1], \\ \ell_{\alpha,f} &= \frac{1}{|D_A|} \sum_{x_A \in D_A} [\|d_{\text{feat}}(x_{AB}) - S_B\|_1], \end{aligned} \quad (8)$$

329 where $d_{\text{feat}}(x)$ represents the domain-specific features pre-
 330 dicted from input x by discriminator d . The discriminator
 331 d minimizes the $\ell_{\alpha,r}$ to learn to reconstruct correct domain-
 332 specific features from real images, and the $g \circ \beta$ network
 333 minimizes the $\ell_{\alpha,f}$ to generate image containing correct
 334 style feature in the target domain.

335 **Image reconstruction loss** We use two kinds of reconstruc-
 336 tion losses here. (1) Self-reconstruction loss, which is to
 337 minimize the L1 norm between x_A and $x_{AA} = g(x_A^i, x_A^s)$.
 338 With such a loss, after given the domain-specific features
 339 x_A^s extracted by $\alpha(\cdot)$, we can ensure what $\beta(\cdot)$ extracts
 340 is the domain-independent features. (2) Cross-domain loss,
 341 which is to minimize the L1 norm between x_A and $x_{ABA} =$
 342 $g(\beta(x_{AB}), x_A^s)$. Thus, the image level reconstruction loss is:

$$\ell_{\text{im}} = \frac{1}{|D_A|} \sum_{x_A \in D_A} [\|x_A - x_{AA}\|_1 + \|x_A - x_{ABA}\|_1]. \quad (9)$$

343 **Overall training loss** We combine the above three losses to
 344 optimize the framework. To optimize the domain-
 345 independent feature extractor $\beta(\cdot)$ and generator g (remind
 346 that α is fixed), we will minimize

$$\ell_{\text{net}}^{\text{total}} = \ell_{\text{GAN}} + \lambda_f \ell_{\alpha,f} + \lambda_{\text{im}} \ell_{\text{im}}. \quad (10)$$

347 To optimize the discriminator, we need to minimize

$$\ell_d^{\text{total}} = -\ell_{\text{GAN}} + \lambda_f \ell_{\alpha,r}, \quad (11)$$

348 where λ_f and λ_{im} are weights to achieve balance among
 349 different loss terms.

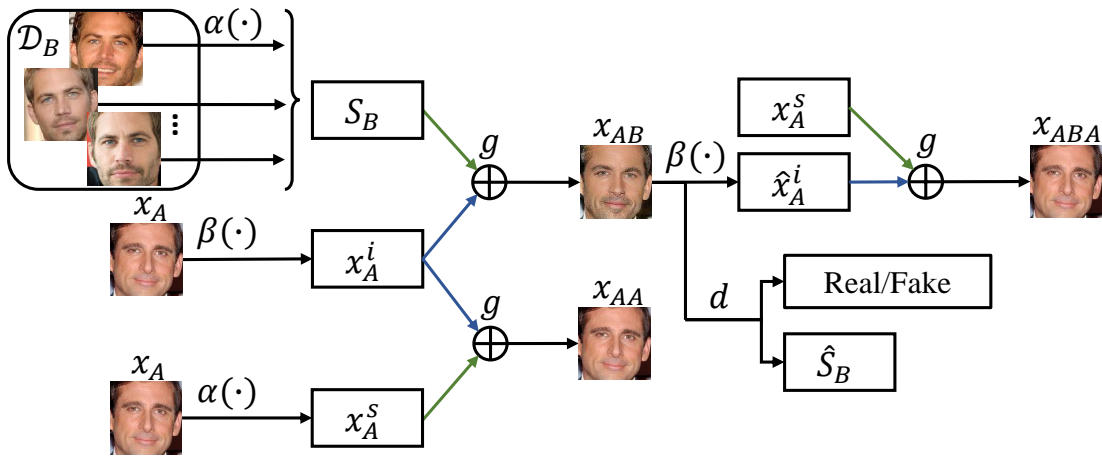


Fig. 2. Training architecture of the proposed DosGAN for unpaired image-to-image translation.

3.4 Architecture for conditional image-to-image translation

The architecture of DosGAN for conditional image-to-image translation (DosGAN-c) is shown in Figure 3. As can be seen, to translate an image x_A from domain A to domain B conditioned on an image x_B from domain B, we first apply the domain-specific feature extractor $\alpha(\cdot)$ on x_B and obtain the domain-specific feature x_B^s . Then we apply the domain-independent feature extractor $\beta(\cdot)$ to x_A and obtain the domain-independent features x_A^i . After that, the generator g takes x_A^i and x_B^s as inputs and generates the translation results x_{AB} . Similarly, x_{BA} is also generated. A mathematical definition is in Definition 2. In this setting, for ease of reference, we set $|D_A| = |D_B|$.

Adversarial loss Similar to non-conditional setting, we illustrate the adversarial loss as below:

$$\ell_{\text{GAN}}^c = \frac{1}{|D_A|} \sum_{x_A \in D_A} \log(d_{\text{adv}}(x_A)) + \log(1 - d_{\text{adv}}(x_{AB})) + \frac{1}{|D_B|} \sum_{x_B \in D_B} \log(d_{\text{adv}}(x_B)) + \log(1 - d_{\text{adv}}(x_{BA})). \quad (12)$$

Domain-specific reconstruction loss Different from non-conditional setting, the domain-specific feature reconstruction cost $\ell_{\alpha,r}$ of real images and $\ell_{\alpha,f}$ of fake images are modified as follows:

$$\begin{aligned} \ell_{\alpha,r}^c &= \frac{1}{|D_A|} \sum_{x_A \in D_A} [\|d_{\text{feat}}(x_A) - x_A^s\|_1] \\ &\quad + \frac{1}{|D_B|} \sum_{x_B \in D_B} [\|d_{\text{feat}}(x_B) - x_B^s\|_1], \\ \ell_{\alpha,f}^c &= \frac{1}{|D_B|} \sum_{\substack{x_A \in D_A \\ x_B \in D_B}} [\|d_{\text{feat}}(x_{AB}) - x_B^s\|_1 \\ &\quad + \|d_{\text{feat}}(x_{BA}) - x_A^s\|_1]. \end{aligned} \quad (13)$$

The discriminator d minimizes the $\ell_{\alpha,r}^c$ to learn to reconstruct correct domain-specific features from real images, and the $g \circ \beta$ network minimizes the $\ell_{\alpha,f}^c$ to generate image containing correct domain-specific features from image in the target domain.

Image reconstruction loss Similar to the non-conditional image-to-image translation, the reconstructed images are defined as follows:

$$\begin{aligned} x_{AA} &= g(x_A^i, x_A^s); x_{BB} = g(x_B^i, x_B^s); \\ x_{ABA} &= g(\beta(x_{AB}), x_A^s); x_{BAB} = g(\beta(x_{BA}), x_B^s). \end{aligned} \quad (14)$$

Correspondingly, the reconstruction loss is

$$\begin{aligned} \ell_{\text{im}}^c &= \frac{1}{|D_A|} \sum_{\substack{x_A \in D_A \\ x_B \in D_B}} [\|x_A - x_{AA}\|_1 + \|x_A - x_{ABA}\|_1 \\ &\quad + \|x_B - x_{BB}\|_1 + \|x_B - x_{BAB}\|_1]. \end{aligned} \quad (15)$$

Overall training loss The total training loss of the generation network and discriminator are defined as follows:

$$\ell_{\text{net}}^{\text{total},c} = \ell_{\text{GAN}}^c + \lambda_f \ell_{\alpha,f}^c + \lambda_{\text{im}} \ell_{\text{im}}^c, \quad (16)$$

$$\ell_d^{\text{total},c} = -\ell_{\text{GAN}}^c + \lambda_f \ell_{\alpha,r}^c, \quad (17)$$

where λ_f and λ_{im} are weights to achieve balance among different loss terms. The $g \circ \beta$ and d should try to minimize $\ell_{\text{net}}^{\text{total},c}$ and $\ell_d^{\text{total},c}$ respectively. The overall process is summarized in Algorithm 1.

3.5 Discussion

Our proposed framework can learn to extract the domain-independent features and combine them with domain-specific features in one single encoder-decoder network.

Take the conditional DosGAN as an example. Consider the path of $x_A \rightarrow \beta(\cdot) \rightarrow (x_A^i, x_A^s) \rightarrow g \rightarrow x_{AA}$ and path of $x_A \rightarrow \beta(\cdot) \rightarrow (x_A^i, x_B^s) \rightarrow g \rightarrow x_{AB}$. Our training objective requires that x_{AA} is an image in domain D_A and x_{AB} is an image in domain D_B . Given the fact that differences between x_{AA} and x_{AB} lay in the differences between x_A^s and x_B^s , thus it is implied that x_A^s and x_B^s are domain-specific features and are extracted by a pre-trained domain-specific feature extractor $\alpha(\cdot)$. Compared with [7], [8], [9], the domain-specific features in our model are extracted by a well-defined and fixed domain classification network, which avoids the feature ambiguity when both domain-specific feature and domain-independent feature extractors

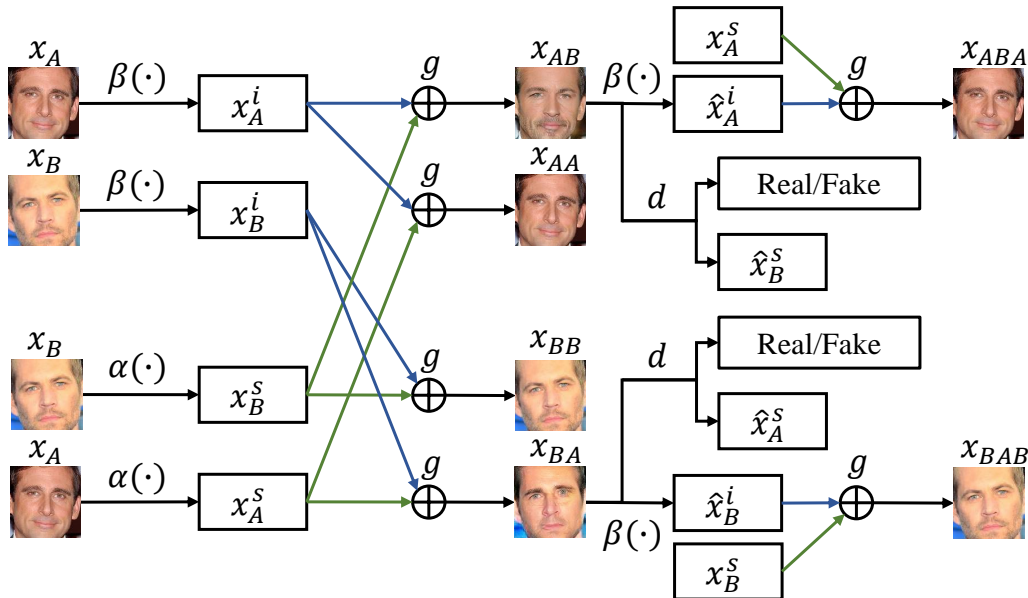


Fig. 3. Training architecture of the proposed DosGAN for unpaired conditional image-to-image translation (briefly, DosGAN-c).

Algorithm 1 DosGAN/DosGAN-c training process.

- 1: *Input:* N image domains $\mathcal{D}_k \forall k \in [N]$, batch size K , learning rate η ;
- 2: Randomly initialize the parameters Θ_α of domain-specific feature extractor $\alpha(\cdot)$.
- 3: Randomly select one domain $\mathcal{D}_k, k \in [N]$. Get a mini-batch of data D_k satisfying $D_k \subset \mathcal{D}_k$ and $|D_k| = K$;
- 4: **Update the classifier** as follows:

$$\Theta_\alpha \leftarrow \Theta_\alpha - \eta \nabla_{\Theta_\alpha} \frac{-1}{|D_k|} \sum_{x \in D_k} \log P(k|x; \Theta_\alpha);$$
- 5: Repeat step 3 and step 4 until convergence.
- 6: Randomly initialize the parameters $\Theta_{go\beta}$ of g and $\beta(\cdot)$, and parameters Θ_d of discriminator d ;
- 7: Randomly select two different domains $\mathcal{D}_A, \mathcal{D}_B, A, B \in [N]$. For each selected domain \mathcal{D}_l where $l \in \{A, B\}$, get a minibatch of data D_l satisfying $D_l \subset \mathcal{D}_l$ and $|D_l| = K$.
- 8: **if** Training DosGAN **then**
- 9: Update the parameters as follows:

$$\begin{aligned} \Theta_{go\beta} &\leftarrow \Theta_{go\beta} - \eta \nabla_{\Theta_{go\beta}} \ell_{net}^{\text{total}}(D_A), \\ \Theta_d &\leftarrow \Theta_d - \eta \nabla_{\Theta_d} \ell_d^{\text{total}}(D_A), \end{aligned} \quad (18)$$

- 10: where $\ell_{net}^{\text{total}}(D_A)$ and $\ell_d^{\text{total}}(D_A)$ are defined in Eqn. (10) and Eqn. (11) respectively.
- 11: **end if**
- 12: **if** Training DosGAN-c **then**
- 13: Update the parameters as follows:

$$\begin{aligned} \Theta_{go\beta} &\leftarrow \Theta_{go\beta} - \eta \nabla_{\Theta_{go\beta}} \ell_{net}^{\text{total},c}(D_A, D_B), \\ \Theta_d &\leftarrow \Theta_d - \eta \nabla_{\Theta_d} \ell_d^{\text{total},c}(D_A, D_B), \end{aligned} \quad (19)$$

- 14: where $\ell_{net}^{\text{total},c}(D_A, D_B)$ and $\ell_d^{\text{total},c}(D_A, D_B)$ are defined in Eqn. (16) and Eqn. (17) respectively.
- 15: **end if**
- 16: Repeat step 7 and step 13 until convergence.

are trained together. With domain-specific features being given, x_A^i should try to inherit the features in x_{AA} and x_{AB} , which is further constrained with reconstruction loss ℓ_{im}^c . Compared with StarGAN [10] that is trained to reconstruct the source input with source domain code, which may cause a semi-optimum when images in one domain vary their own characteristic very much, such as the same identity may have different face appearance at different time, our model is trained with features from real images in every training step, and ideally can accurately reconstruct source input with its own domain-specific features.

4 EXPERIMENTS

4.1 Implementation details

In the following experiments, our DosGAN/DosGAN-c's network configuration is shown in Figure 4. For $\alpha(\cdot)$, it consists of one convolution layer with stride 1 and kernel size 4×4 ; six convolution layers with stride 2 and kernel size 4×4 ; the last two convolution layers that are implemented for domain-specific feature output and classification output. The number of domain-specific features is set to 1024 for multiple identity translation and multiple facial attribute translation, 64 for multiple season translation, 16 for conditional cross-domain translation according to different tasks' domain classification accuracy and feature compactness. For discriminator d , we use PatchGANs [20] that consists of six convolution layers with stride 2 and kernel size 4×4 , and two separated convolution layers that are implemented for discrimination output $d_{adv}(x)$ and domain-specific feature reconstruction output $d_{feat}(x)$. For $\beta(\cdot)$, it one convolution layer with stride 1 and kernel size 7×7 , two convolution layers with stride 2 and kernel size 4×4 , and 3 residual blocks [32]. Each convolution layer is followed by Instance Normalization (IN) [33] and ReLU units [34]. For generator g , it first processes the domain-specific features through a fully-connected layer and adds it to domain-independent features from encoder e . Then the combined feature is input

438 to 3 residual blocks, two deconvolution layers with stride 2
 439 and kernel size 3×3 followed by IN and ReLU units, and
 440 one convolution layer with stride 1 and kernel size 7×7 .

441 We set the parameters $\lambda_f = 5$ for multiple identity trans-
 442 lation and multiple facial attribute translation, $\lambda_f = 0.15$ for
 443 multiple season translation, $\lambda_f = 0.5$ for conditional cross-
 444 domain translation, and $\lambda_{im} = 10$ for all the experiments.
 445 We train our networks using Adam [35] with learning rate of
 446 0.0001. For all experiments, we train models with a learning
 447 rate of 0.0001 in the first 100000 iterations and linearly
 448 decay the learning every 1000 iteration.

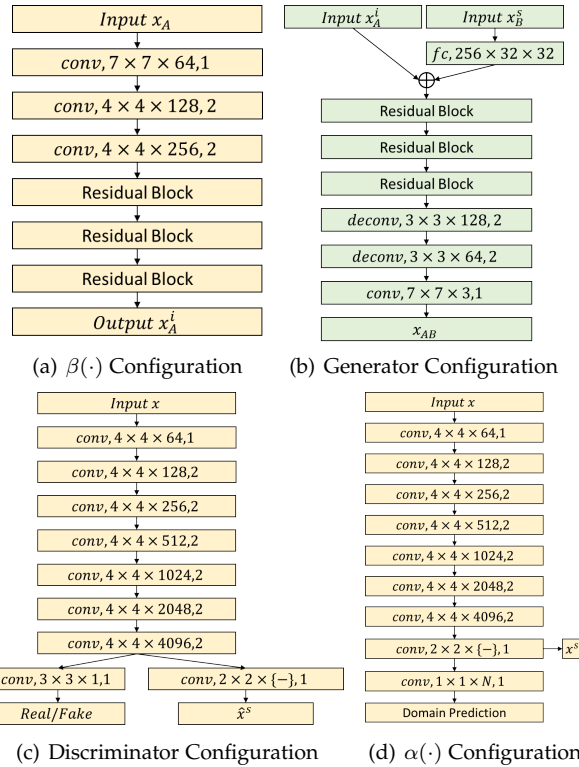


Fig. 4. The network configuration of DosGAN/DosGAN-c. $\{-\}$ represents the number of domain-specific features which is determined by the different tasks.

4.2 Baselines

To verify the generality of our model, we compare with four state-of-the-art image translation models for different image-to-image translation tasks.

CycleGAN [6], [12], [27]. CycleGAN was proposed for cross-domain translation task, which jointly trains two mappings with adversarial loss and dual loss.

BicycleGAN [23]. BicycleGAN was proposed for multimodal cross-domain translation and learns to combine input image with latent code. We compare with BicycleGAN when the paired data is available.

cd-GAN [7]. cd-GAN was proposed for unpaired conditional cross-domain translation, which aims to translate an image from source domain conditioned on a given image in the target domain. We show that our model can also deal with this problem.

StarGAN [10]. StarGAN can perform multi-domain translation using a single model. We compare with StarGAN in the case of multi-domain translation.

MUNIT [8] and DRIT [9]. Both works are proposed for unpaired multimodal cross-domain translation, and learn to disentangle latent space and generate diverse translation results.

4.3 Datasets

For multi-domain translation, we compare our model with StarGAN on multiple facial attribute (three hair colors, including black hair, blond hair, brown hair; two genders, including male and female; two ages, including old and young) translation on CelebA dataset [36], multiple season translation and multiple identity translation on both Face-scrub dataset [37] and CelebA.

For multiple facial attribute translation, the initial images in CelebA whose sizes are 178×218 are resized to 128×156 . The test set is built by randomly selecting 2000 images from the original dataset. All the remaining images are used as the training set.

For multiple season translation, the season dataset [38] consists of approximately 6000 images and are categorized into four seasons, i.e., Spring, Summer, Autumn and Winter. All images are resized to 256×256 .

For multiple identity translation, the Facescrub dataset [37] comprises more than 100 thousands face images of 531 male and female celebrities, with about 200 images per person. We resize all face images to 128×128 and obtain 531 identity domains. We build the test set by randomly selecting 20 images per person from the original dataset. All the remaining images are used as the training set. The face images of CelebA dataset contains 10177 identities but do not have corresponding identity labels. We apply a cropping box (25, 60, 133, 168) on CelebA images and resize them to 128×128 .

For conditional cross-domain translation [7], we carry out experiments on edges→shoes dataset [39] and edges→handbags dataset [40].

4.4 Multiple identity translation

We conduct multiple identity translation with DosGAN and conditional DosGAN (briefly, DosGAN-c) as illustrated in Eqn. (5) and Eqn. (6) respectively. Given random inputs and target identities in conditional inputs, the results of multiple identity translation compared with StarGAN [10] are shown in Figure 5. In general, our proposed method can successfully transfer the identity of input image to identity of the conditional input and greatly outperforms StarGAN. There are several aspects of observation.

(1) Results of our DosGAN are much visually better than StarGAN's. One main reason may be that using manually-set domain code without semantic meaning for domain representation is inappropriate and insufficient for multiple domain translation, especially when the domain number is large (i.e., $N = 531$). On the contrary, our results are generated by combining domain-independent features and domain-specific features which are well disentangled and are both from real image inputs. Therefore, our model does not need to learn to relate domain code with corresponding identity of each image, but only needs to focus on generating results with two kinds of well-defined features.

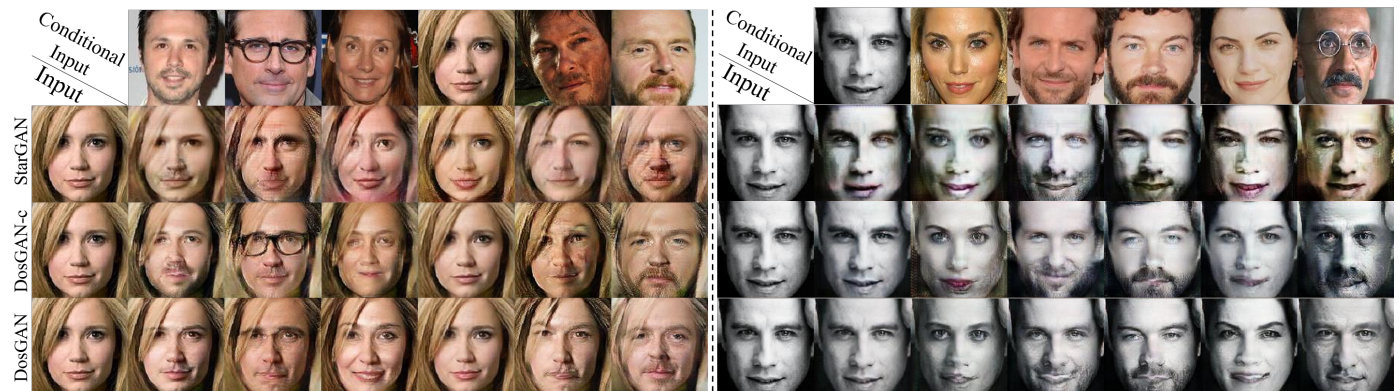


Fig. 5. Multiple identity translation results of StarGAN and our DosGAN on Facescrub. The first column is inputs x_A , and the first row is x_B for DosGAN-c's conditional inputs and target identity examples for StarGAN and DosGAN. Other images are the translation results.

TABLE 1

Top-1 and top-5 face recognition accuracy [%] of multiple identity translation results on Facescrub.

	StarGAN [10]	DosGAN-c	DosGAN	Real Faces
Top-1	55.04	60.79	<u>94.01</u>	80.20
Top-5	71.34	75.92	97.98	95.13

(2) Our DosGAN-c can translate not only the input to the target identity, but also the specific face details (such as makeup, eyeglass) in the conditional input, while StarGAN can only translate input to the deterministic output without specific details.

(3) Both DosGAN and DosGAN-c can more accurately reconstruct the original inputs x_A than StarGAN as the images at the fifth column in the left figure and the first column in the right figure. This is because StarGAN is required to reconstruct the original image with original domain code, but domain code for the same identity may have different face appearance at different time, which causes a relatively hard optimization for reconstruction accuracy. Our domain-specific features can effectively avoid this problem since the reconstruction of x_A is generated by domain-specific features from itself.

For quantitative evaluation, we argue that if images translated by a model are accurately classified as the target identity's classes, the model is successful on multiple identity translation. We translate source image to random target identity in each test minibatch, and report the top-1 and top-5 face recognition accuracy of generated images from StarGAN and our model in Table 1 with re-trained VGG-16 network [41]. We can see that our proposed method achieves better face recognition accuracy than StarGAN in both settings.

We also surprisingly find that the classification accuracy of images generated by DosGAN is much higher than that of real faces in the test set. To explain this phenomenon, we split the training set into two parts: One is used to train the classifier VGG-16 (briefly denoted as $VGG-16_{half}$), and the other is used to train DosGAN (briefly denoted as $DosGAN_{half}$). The face recognition accuracy of two VGG-16s, that are trained on full training set and half training set respectively, on training images, testing images, generated

TABLE 2

Top-1 face recognition accuracy [%] of two VGG-16s, that are trained on full training set and half training set respectively, on training images, testing images, generated images from DosGAN and generated images from $DosGAN_{half}$.

	Training Faces	Testing Faces	DosGAN	$DosGAN_{half}$
$VGG-16$	99.68	80.20	94.01	—
$VGG-16_{half}$	99.53	78.42	—	80.98

images from two DosGANs is shown in Table 2. We can find that when $VGG-16$ and DosGAN are trained with different training sets, classification accuracy of generated images from $DosGAN_{half}$ (80.98%) is only slightly higher than testing images's (78.42%). This is because our model can effectively make use of training images' domain-specific features and carry the learned features for image generation in the testing phase (we take the expectation over domain-specific features from all training images as the domain characteristics). Therefore, when DosGAN and $VGG-16$ are trained with same dataset, DosGAN will generate images that have similar characteristics like training images and cause a similar classification accuracy as training images. Even for $VGG-16_{half}$, our model has higher accuracy than test images since a generated image containing the expectation of domain features is more capable to present the special characteristics of an identity than a single image.

4.5 Adapting translation from Facescrub to CelebA

Most existing image-to-image translation works focus on translation within dataset that has clear domain information. However, there are still many datasets that does not contain domain information. An example is CelebA: for any photo in CelebA, we do not know which identity this photo belongs to. As far as we know, no previous work has touched how to achieve translation on dataset without domain separation, since there is no way to extract domain-specific features.

Considering both CelebA and Facescrub are face datasets, we can transfer the $\alpha(\cdot)$ trained on Facescrub to that for CelebA, and then retrain the $\beta(\cdot)$ and g in the DosGAN-c for CelebA to achieve conditional image-to-image translation. The basic assumption on this translation



Fig. 6. Our results on multiple identity translation on unlabeled CelebA with domain supervision from Facescrub.

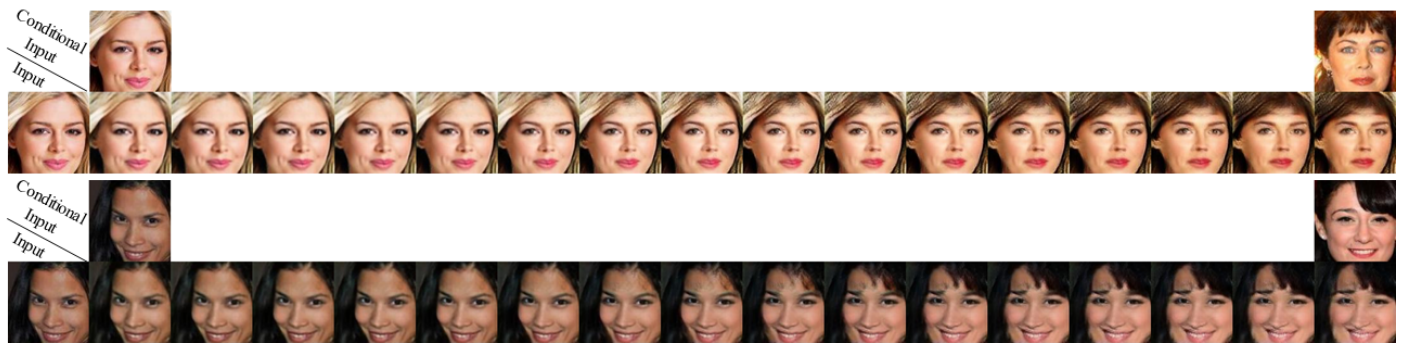


Fig. 7. Domain-specific interpolations on the CelebA. The translation results are generated by combining input's domain-independent features with domain-specific features interpolated linearly from left conditional input's to right conditional input's.

transferring is that the two datasets share the same semantic representations (i.e., face images), the $\alpha(\cdot)$ trained on Face-scrub provides a viable way to estimate the domain-specific features for the faces in the CelebA. The results of multiple identity translation on CelebA are shown in Figure 6. We can observe that our model can still successfully translate the identity of input to the identity of conditional input with invariant domain-independent features (i.e., face emotion, face orientation).

To verify the disentanglement of domain-independent features and domain-specific features, we show the results of domain-specific feature interpolations in Figure 7. We sample two conditional inputs x_{B1} and x_{B2} and obtain their domain-specific features x_{B1}^s and x_{B2}^s . Then we linearly interpolate between x_{B1}^s and x_{B2}^s and combine intermediary feature with domain-independent features of input x_A . We observe that our model can produce smooth translations through variation of domain-specific feature while remaining the domain-independent features invariant. This indicates that DosGAN-c learns not only individual translation with specific real images, but also a generalized domain-specific feature distribution.

4.6 Adapting translation to unseen domains

To further evaluate the transferability of DosGAN-c, we choose 528 of 531 identities in Facescrub as the dataset with domain information, and the rest 3 identities are shuffled and used as dataset without domain information. We train



Fig. 8. Our results on multiple identity translation on 3 identities in Facescrub with domain supervision from 528 identities in Facescrub.

TABLE 3
Top-1 and top-5 face recognition accuracy [%] of 3 identities identity translation results on Facescrub.

	StarGAN [10]	DosGAN-c
Top-1	6.75	58.46
Top-5	20.77	73.55

the StarGAN and our DosGAN-c on 528 identities. Then we directly test the two models on the rest 3 identities, without any further tuning like that in Section 4.5. The domain codes of StarGAN for unknown 3 identities are provided based on the prediction of classifier trained on 528 identities. The translation examples on 3 identities are shown in Figure 8. The face recognition accuracy of translation results on 3 identities are shown in Table 3.

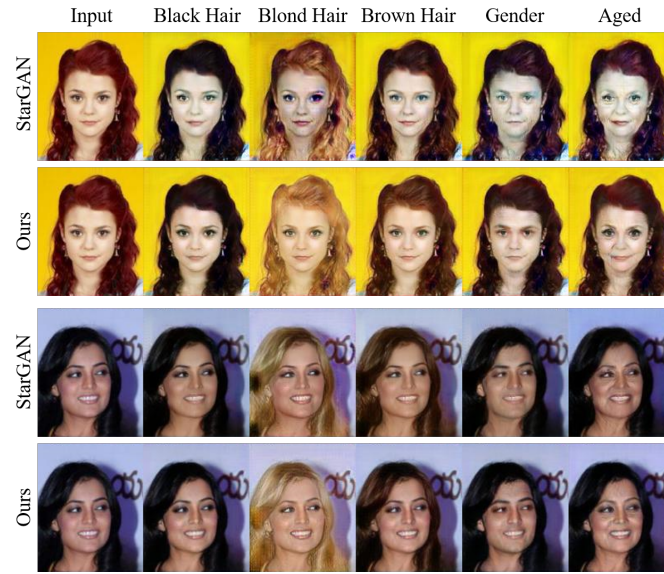


Fig. 9. Comparison between StarGAN and our DosGAN on multiple facial attribute translation.

We can observe that performance of StarGAN decreases rapidly and StarGAN can not generalize its model to image translation that contains unseen domains. On the contrary, given pre-trained classifier, our model does not need any other additional information to deal with unseen identities, and shows consistent performance on image translation across different datasets.

TABLE 4
Classification error rate on multiple facial attribute translation.

	Hair Color	Gender	Age
StarGAN [10]	19.01%	11.60%	25.52%
Ours	17.56%	11.12%	23.79 %

633

4.7 Multiple facial attribute translation

To further verify the effectiveness of our DosGAN on non-conditional setting, we compare with StarGAN on multiple facial attribute translation as shown in Figure 9. We can observe that our model can ensure more consistency of domain-independent features in the translated results than StarGAN. For example, in the top part of Figure 9, faces generated by StarGAN are found to contain more noise than our model. In addition, our model can also produce more accurate domain-specific features in the translated results than StarGAN. For example, in the bottom part of Figure 9, the blond hair generated by StarGAN is not very pure and has little brown color. We also show the classification error rate of translation results in Table 4. We can see that our model achieves lower classification error rate than StarGAN on three different domains, which corresponds with qualitative results.

4.8 Multiple season translation

We also carry out multi-domain translation on multiple season translation task. This task aims to demonstrate the effectiveness of DosGAN on generating higher resolution images

TABLE 5
FID scores of multiple season translation.

	StarGAN [10]	DosGAN	Improvement
FID	81.81	51.14	30.67

and natural images. The translation results compared with StarGAN are shown in Figure 10. Compared with StarGAN, we can observe that our model can translate the input images to the target domain with more accurate details and higher quality. For example, the translated results of our DosGAN have more clear edges, precisely contain most season features, remain other season-invariant features, such as the waterfall. We also present the Frchet Inception Distance (FID) [42] scores of StarGAN and DosGAN in Table 5. The FID scores verify our model's significant improvement on StarGAN.

4.9 Conditional cross-domain translation results

To further investigate the effectiveness of our DosGAN-c on conditional image-to-image setting, we compare our model with CycleGAN [6], DRIT [9], MUNIT [8], BicycleGAN [23] and cd-GAN [7] on conditional edges→handbags and edges→shoes. The conditional translation results are shown in Figure 11. In order to measure the accuracy of domain-specific features in translation results, we present the quantitative comparison results in Table 6, where we calculate Peak Signal to Noise Ratio (PSNR), Structural Similarity (SSIM), FID score between ground truth images and translated images generated from paired edge images (providing domain-independent features) and ground truth shoe/handbag images (providing domain-specific features). From Figure 11, we show that our model can visually transfer the domain-specific features from the conditional input to the translation result. The quantitative results in Table 6 further verify that our model's performance is better than cd-GAN, DRIT, MUNIT and comparable with supervised model BicycleGAN.

In addition to objective measurements, we carry out human perceptual study to further evaluate our results. The reviewers are given an input image and two translated images from two different methods, and they have to choose the better one without knowing which method the images are generated from. We randomly select 100 groups of images for each compared method. The User Study (UR) statistics are also shown in Table 6. We can observe that our model achieves the best user study result among the unsupervised image-to-image models.

4.10 Ablation study

To verify the effectiveness of the image reconstruction loss ℓ_{im} , domain-specific reconstruction loss $\ell_{\alpha,f}$ and pre-training strategy, we quantitatively compare DosGAN with four variants on the multiple identity translation. Two variants of DosGAN ablate ℓ_{im} and $\ell_{\alpha,f}$. The other one variant (briefly denoted as DosGAN_f) replaces d_{feat} with α in Eqn. (8), omits the $\ell_{\alpha,r}$ loss and only optimizes the new $\ell_{\alpha,f}$ loss

$$\ell_{\alpha,f} = \frac{1}{|D_A|} \sum_{x_A \in D_A} [\|\alpha(x_{AB}) - S_B\|]. \quad (20)$$

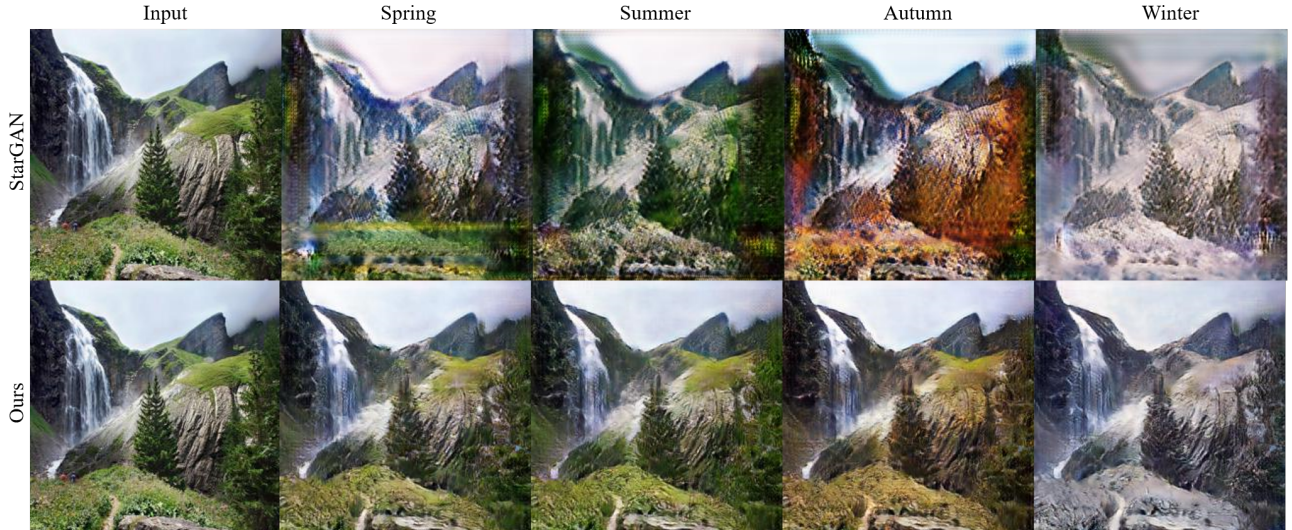


Fig. 10. Comparison between StarGAN and our DosGAN on multiple season translation.



Fig. 11. Comparison among CycleGAN, cd-GAN, DRIT, MUNIT, BicycleGAN and our DosGAN-c on conditional edges→handbags (a) and edges→shoes (b) translation. The conditional input provides domain-specific features to the translation result.

TABLE 6

PSNR [dB], SSIM, FID between ground truth images and translation images generated from paired edge images and ground truth images. The UR is the user study statistics. ↑ means the larger score is better. ↓ means the lower score is better.

	edges→handbags				edges→shoes			
	PSNR↑	SSIM↑	FID↓	US↑	PSNR↑	SSIM↑	FID↓	US↑
CycleGAN [6]	8.45	0.3446	86.40	21.3%	13.23	0.5028	75.54	23.4%
cd-GAN [7]	16.05	0.6590	84.50	43.5%	17.85	0.7149	80.73	45.2%
DRIT [9]	11.49	0.5139	98.27	38.1%	16.49	0.7226	84.64	42.7%
MUNIT [8]	14.54	0.6440	79.32	44.2%	17.95	0.7353	70.72	48.7%
BicycleGAN [23] (Supervised)	16.65	0.6779	75.59	54.8%	18.95	0.7605	70.81	56.9%
DosGAN-c	16.47	0.6620	78.67	50.0%	18.02	0.7376	71.22	50.0%

The another one variant (briefly denoted as DosGAN_p)
705 optimize all network components together instead of pre-
706 training $\alpha(\cdot)$. Without touching ℓ_d^{total} , $\alpha(\cdot)$, $\beta(\cdot)$ and g are
707 optimized by a new loss $\ell_{\text{net}}^{\text{total}}$:

$$\ell_{\text{net}}^{\text{total}} = \ell_{\text{GAN}} + \ell_{\text{cls}} + \lambda_f \ell_{\alpha,f} + \lambda_{\text{im}} \ell_{\text{im}}, \quad (21)$$

$$\ell_{\text{cls}} = -P(l = A|x_A; \alpha(\cdot)). \quad (22)$$

TABLE 7
Ablation study of DosGAN on multiple identity translation.

	Top-1 (%)	Top-5 (%)
DosGAN w/o ℓ_{im}	55.28	70.19
DosGAN w/o $\ell_{\alpha,f}$	11.16	13.28
DosGAN _f	15.99	20.52
DosGAN _p	61.21	77.32
DosGAN	94.01	97.98

As shown in Table 7, removing ℓ_{im} and $\ell_{\alpha,f}$ from DosGAN leads to significantly worse classification accuracy rate. In addition, the DosGAN_f also fails to translate images as DosGAN, which indicates that the necessity of the $\ell_{\alpha,f}$ and $\ell_{\alpha,r}$ to DosGAN's training. Without pre-training, DosGAN_p also shows performance degradation compared with original model, which verifies that an explicitly formulated domain classifier can lead to better factor disentanglement of domain-specific features and domain-independent features.

5 CONCLUSIONS

In this paper, we have presented a novel framework called DosGAN/DosGAN-c to utilize domain information as explicit supervision for unconditional or conditional image-to-image translation. The effectiveness of our approach has been demonstrated on cross-domain and multi-domain image translation tasks. Moreover, the pre-trained domain-specific feature extractor can be transferred to other datasets without domain supervision information.

There are several interesting future directions. First, we can apply our model to more image translation tasks. Second, we would like to explore how to use our techniques for zero-shot image-to-image translation. Furthermore, we believe that our framework can be generalized to other tasks such as language and speech.

REFERENCES

- [1] Leon A Gatys, Alexander S Ecker, and Matthias Bethge. Image style transfer using convolutional neural networks. In *Proceedings of the IEEE Conference on Computer Vision and Pattern Recognition*, pages 2414–2423, 2016.
- [2] Jonathan Long, Evan Shelhamer, and Trevor Darrell. Fully convolutional networks for semantic segmentation. In *Proceedings of the IEEE Conference on Computer Vision and Pattern Recognition*, pages 3431–3440, 2015.
- [3] C. Ledig, L. Theis, F. Huszár, J. Caballero, A. Cunningham, A. Acosta, A. Aitken, A. Tejani, J. Totz, Z. Wang, and W. Shi. Photo-realistic single image super-resolution using a generative adversarial network. In *2017 IEEE Conference on Computer Vision and Pattern Recognition (CVPR)*, pages 105–114, July 2017.
- [4] Ian Goodfellow, Jean Pouget-Abadie, Mehdi Mirza, Bing Xu, David Warde-Farley, Sherjil Ozair, Aaron Courville, and Yoshua Bengio. Generative adversarial nets. In *Advances in neural information processing systems*, pages 2672–2680, 2014.
- [5] Di He, Yingce Xia, Tao Qin, Liwei Wang, Nenghai Yu, Tieyan Liu, and Wei-Ying Ma. Dual learning for machine translation. In *Advances in Neural Information Processing Systems*, pages 820–828, 2016.
- [6] Jun-Yan Zhu, Taesung Park, Phillip Isola, and Alexei A. Efros. Unpaired image-to-image translation using cycle-consistent adversarial networks. In *The IEEE International Conference on Computer Vision (ICCV)*, Oct 2017.
- [7] Jianxin Lin, Yingce Xia, Tao Qin, Zhibo Chen, and Tie-Yan Liu. Conditional image-to-image translation. In *Proceedings of the IEEE Conference on Computer Vision and Pattern Recognition*, 2018.
- [8] Xun Huang, Ming-Yu Liu, Serge Belongie, and Jan Kautz. Multi-modal unsupervised image-to-image translation. In *ECCV*, 2018.
- [9] Hsin-Ying Lee, Hung-Yu Tseng, Jia-Bin Huang, Maneesh Kumar Singh, and Ming-Hsuan Yang. Diverse image-to-image translation via disentangled representations. In *European Conference on Computer Vision*, 2018.
- [10] Yunjey Choi, Minje Choi, Munyoung Kim, Jung-Woo Ha, Sunghun Kim, and Jaegul Choo. Stargan: Unified generative adversarial networks for multi-domain image-to-image translation. In *The IEEE Conference on Computer Vision and Pattern Recognition (CVPR)*, June 2018.
- [11] Alexander H. Liu, Yen-Cheng Liu, Yu-Ying Yeh, and Yu-Chiang Frank Wang. A unified feature disentangler for multi-domain image translation and manipulation. In S. Bengio, H. Wallach, H. Larochelle, K. Grauman, N. Cesa-Bianchi, and R. Garnett, editors, *Advances in Neural Information Processing Systems 31*, pages 2595–2604. Curran Associates, Inc., 2018.
- [12] Zili Yi, Hao Zhang, Ping Tan, and Minglun Gong. Dualgan: Unsupervised dual learning for image-to-image translation. In *The IEEE International Conference on Computer Vision (ICCV)*, Oct 2017.
- [13] Alec Radford, Luke Metz, and Soumith Chintala. Unsupervised representation learning with deep convolutional generative adversarial networks. *arXiv preprint arXiv:1511.06434*, 2015.
- [14] Emily L Denton, Soumith Chintala, Rob Fergus, et al. Deep generative image models using a laplacian pyramid of adversarial networks. In *Advances in neural information processing systems*, pages 1486–1494, 2015.
- [15] Paul Smolensky. Information processing in dynamical systems: Foundations of harmony theory. Technical report, COLORADO UNIV AT BOULDER DÉPT OF COMPUTER SCIENCE, 1986.
- [16] Geoffrey E Hinton and Ruslan R Salakhutdinov. Reducing the dimensionality of data with neural networks. *science*, 313(5786):504–507, 2006.
- [17] Pascal Vincent, Hugo Larochelle, Yoshua Bengio, and Pierre-Antoine Manzagol. Extracting and composing robust features with denoising autoencoders. In *Proceedings of the 25th international conference on Machine learning*, pages 1096–1103. ACM, 2008.
- [18] Diederik P Kingma and Max Welling. Auto-encoding variational bayes. *arXiv preprint arXiv:1312.6114*, 2013.
- [19] Xi Chen, Yan Duan, Rein Houthooft, John Schulman, Ilya Sutskever, and Pieter Abbeel. Infogan: Interpretable representation learning by information maximizing generative adversarial nets. In *Advances in Neural Information Processing Systems*, pages 2172–2180, 2016.
- [20] P. Isola, J. Zhu, T. Zhou, and A. A. Efros. Image-to-image translation with conditional adversarial networks. In *2017 IEEE Conference on Computer Vision and Pattern Recognition (CVPR)*, pages 5967–5976, July 2017.
- [21] Ting-Chun Wang, Ming-Yu Liu, Jun-Yan Zhu, Andrew Tao, Jan Kautz, and Bryan Catanzaro. High-resolution image synthesis and semantic manipulation with conditional gans. In *Proceedings of the IEEE Conference on Computer Vision and Pattern Recognition*, 2018.
- [22] Joshua B Tenenbaum and William T Freeman. Separating style and content with bilinear models. *Neural computation*, 12(6):1247–1283, 2000.
- [23] Jun-Yan Zhu, Richard Zhang, Deepak Pathak, Trevor Darrell, Alexei A Efros, Oliver Wang, and Eli Shechtman. Toward multimodal image-to-image translation. In *Advances in Neural Information Processing Systems*, pages 465–476, 2017.
- [24] Vincent Dumoulin, Ishmael Belghazi, Ben Poole, Alex Lamb, Martin Arjovsky, Olivier Mastropietro, and Aaron Courville. Adversarially learned inference. *arXiv preprint arXiv:1606.00704*, 2016.
- [25] Jeff Donahue, Philipp Krähenbühl, and Trevor Darrell. Adversarial feature learning. *arXiv preprint arXiv:1605.09782*, 2016.
- [26] Yaniv Taigman, Adam Polyak, and Lior Wolf. Unsupervised cross-domain image generation. *arXiv preprint arXiv:1611.02200*, 2016.
- [27] Taeksoo Kim, Moonsu Cha, Hyunsoo Kim, Jung Kwon Lee, and Jiwon Kim. Learning to discover cross-domain relations with generative adversarial networks. In *Proceedings of the 34th International Conference on Machine Learning*, pages 1857–1865, 2017.
- [28] Shuang Ma, Jianlong Fu, Chang Wen Chen, and Tao Mei. Da-gan: Instance-level image translation by deep attention generative adversarial networks. In *The IEEE Conference on Computer Vision and Pattern Recognition (CVPR)*, June 2018.
- [29] A. Pumarola, A. Agudo, A.M. Martinez, A. Sanfeliu, and F. Moreno-Noguer. Ganimation: Anatomically-aware facial anima-

- tion from a single image. In *Proceedings of the European Conference on Computer Vision (ECCV)*, 2018.
- [30] Youssef Alami Mejati, Christian Richardt, James Tompkin, Darren Cosker, and Kwang In Kim. Unsupervised attention-guided image-to-image translation. In S. Bengio, H. Wallach, H. Larochelle, K. Grauman, N. Cesa-Bianchi, and R. Garnett, editors, *Advances in Neural Information Processing Systems 31*, pages 3697–3707. Curran Associates, Inc., 2018.
- [31] Xinyuan Chen, Chang Xu, Xiaokang Yang, and Dacheng Tao. Attention-gan for object transfiguration in wild images. In *Proceedings of the European Conference on Computer Vision (ECCV)*, pages 164–180, 2018.
- [32] Kaiming He, Xiangyu Zhang, Shaoqing Ren, and Jian Sun. Deep residual learning for image recognition. In *Proceedings of the IEEE conference on computer vision and pattern recognition*, pages 770–778, 2016.
- [33] Dmitry Ulyanov, Andrea Vedaldi, and Victor Lempitsky. Instance normalization: The missing ingredient for fast stylization. *arXiv preprint*, 2016.
- [34] Vinod Nair and Geoffrey E Hinton. Rectified linear units improve restricted boltzmann machines. In *Proc. ICML*, pages 807–814, 2010.
- [35] Diederik Kingma and Jimmy Ba. Adam: A method for stochastic optimization. *arXiv preprint arXiv:1412.6980*, 2014.
- [36] Ziwei Liu, Ping Luo, Xiaogang Wang, and Xiaoou Tang. Deep learning face attributes in the wild. In *Proceedings of International Conference on Computer Vision (ICCV)*, 2015.
- [37] Hong-Wei Ng and Stefan Winkler. A data-driven approach to cleaning large face datasets. In *Image Processing (ICIP), 2014 IEEE International Conference on*, pages 343–347. IEEE, 2014.
- [38] Asha Anoosheh, Eirikur Agustsson, Radu Timofte, and Luc Van Gool. Combogan: Unrestrained scalability for image domain translation. In *Proceedings of the IEEE Conference on Computer Vision and Pattern Recognition Workshops*, pages 783–790, 2018.
- [39] Aron Yu and Kristen Grauman. Fine-grained visual comparisons with local learning. In *Proceedings of the IEEE Conference on Computer Vision and Pattern Recognition*, pages 192–199, 2014.
- [40] Jun-Yan Zhu, Philipp Krähenbühl, Eli Shechtman, and Alexei A Efros. Generative visual manipulation on the natural image manifold. In *European Conference on Computer Vision*, pages 597–613. Springer, 2016.
- [41] Karen Simonyan and Andrew Zisserman. Very deep convolutional networks for large-scale image recognition. *arXiv preprint arXiv:1409.1556*, 2014.
- [42] Martin Heusel, Hubert Ramsauer, Thomas Unterthiner, Bernhard Nessler, and Sepp Hochreiter. Gans trained by a two time-scale update rule converge to a local nash equilibrium. In I. Guyon, U. V. Luxburg, S. Bengio, H. Wallach, R. Fergus, S. Vishwanathan, and R. Garnett, editors, *Advances in Neural Information Processing Systems 30*, pages 6626–6637. Curran Associates, Inc., 2017.

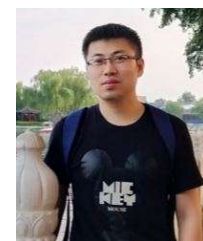
83



Zhibo Chen (M'01-SM'11) received the B. Sc., and Ph.D. degree from Department of Electrical Engineering Tsinghua University in 1998 and 2003, respectively. He is now a professor in University of Science and Technology of China. Before that he has worked in SONY and Thomson from 2003 to 2012. He used to be principal scientist and research manager in Thomson Research & Innovation Department.

His research interests include image and video compression, visual quality of experience assessment, immersive media computing and intelligent media computing. He has more than 50 granted and over 100 filed EU and US patent applications, more than 70 publications and standard proposals. He is IEEE senior member, member of IEEE Visual Signal Processing and Communications Committee, and member of IEEE Multimedia Communication Committee. He was organization committee member of ICIP 2017 and ICME 2013, served as TPC member in IEEE ISCAS and IEEE VCIP.

900
901
902
903
904
905
906
907
908
909
910
911
912
913
914
915
916
917



Yingce Xia is currently an associated researcher at Microsoft Research Asia. He received his Ph.D. degree from University of Science and Technology in 2018, supervised by Dr. Tie-Yan Liu and Prof. Nenghai Yu. Prior to that, he obtained the bachelor degree from University of Science and Technology of China in 2013. His research interests are deep learning and machine learning.

918
919
920
921
922
923
924
925
926
927



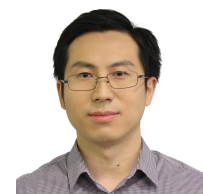
Sen Liu received the B.S. degree in computer science from the Beijing University of Posts and Telecommunications, Beijing, China, in 2013. Currently, he is serving as Associate Researcher at Institute of Advanced Technology, University of Science and Technology of China. His area of interests includes artificial intelligence, deep learning, video coding, computer vision and pattern recognition and reinforcement learning.

928
929
930
931
932
933
934
935
936
937



Jianxin Lin received the B.S. degree in electronic engineering from University of Science and Technology of China in 2015. Now he is pursuing for his Ph.D. degree at University of Science and Technology of China. His research interests include computer vision and machine learning. He has published several papers on CVPR, AAAI, IJCAI, TIP and so on. He also serves as reviewer for ICML-2019, ICME-2019, NeurIPS-2019, AAAI-2020 and so on.

888
889
890
891
892
893
894
895
896
897
898



Tao Qin is a Principal Research Manager at Microsoft Research Asia. His research interests include machine learning (with the focus on deep learning and reinforcement learning), artificial intelligence (with applications to language understanding and games), game theory and multi-agent systems (with applications to cloud computing, online and mobile advertising, e-commerce), information retrieval and computational advertising. His team won eight top places in the recent machine translation challenge organized

938
939
940
941
942
943
944
945
946
947
948
949
950
951

by the fourth Conference on Machine Translation (WMT19). He is a senior member of ACM and IEEE, and an Adjunct Professor (PhD advisor) in the University of Science and Technology of China.

Jiebo Luo (S'93, M'96, SM'99, F'09) joined the Department of Computer Science at the University of Rochester in 2011, after a prolific career of over 15 years with Kodak Research. He has authored over 400 technical papers and holds over 90 U.S. patents. His research interests include computer vision, machine learning, data mining, social media and biomedical informatics. He has served as the Program Chair of the ACM Multimedia 2010, IEEE CVPR 2012, ACM ICMR 2016, and IEEE ICIP 2017, and on the Editorial TRANSACTIONS ON PATTERN ANALYSIS AND
ENCE, IEEE TRANSACTIONS ON MULTIMEDIA,
S ON CIRCUITS AND SYSTEMS FOR VIDEO
TRANSACTIONS ON BIG DATA, Pattern Recog-
nition and Applications, and ACM Transactions on
d Technology. He is also a Fellow of ACM, AAAI,